

# Bayesian Prediction under Moment Conditioning

Nicholas G. Polson<sup>1\*</sup>

<sup>1</sup>Booth School of Business, University of Chicago

Daniel Zantedeschi<sup>2†</sup>

<sup>2</sup>Muma College of Business, University of South Florida

March 20, 2026

## Abstract

Prediction is a central task of statistics and machine learning, yet many inferential settings provide only partial information, typically in the form of moment constraints or estimating equations. We develop a finite, fully Bayesian framework for propagating such partial information through predictive distributions. Building on de Finetti's representation theorem, we construct a curvature-adaptive version of exchangeable updating that operates directly under finite constraints, yielding an explicit discrete-Gaussian mixture that quantifies predictive uncertainty. The resulting finite-sample bounds depend on the smallest eigenvalue of the information-geometric Hessian, which measures the curvature and identification strength of the constraint manifold. This approach unifies empirical likelihood, Bayesian empirical likelihood, and generalized method-of-moments estimation within a common predictive geometry. On the operational side, it provides computable curvature-sensitive uncertainty bounds for constrained prediction; on the theoretical side, it recovers de Finetti's coherence, Doob's martingale convergence, and local asymptotic normality as limiting cases of the same finite mechanism. Our framework thus offers a constructive bridge between partial information and full Bayesian prediction.

*Keywords:* Asymptotic theory; Bayesian inference; constraint geometry; empirical likelihood; exchangeability; information projection; predictive distribution

---

\*ngp@chicagobooth.edu

†danielz@usf.edu

# 1 Introduction

Prediction under constraint lies at the heart of scientific inquiry. Constraints arise in many forms—moment conditions, invariances, sparsity, or limited observability—and pervade modelling practice across the sciences. Whether in econometrics, machine learning, or Bayesian analysis, we often possess only partial information about the system under study. How should such knowledge be operationalized within a coherent probabilistic framework? This question motivates our study of *Bayesian prediction under moment conditioning*.

From a sequential viewpoint, prediction provides the operational meaning of inference: the Bayesian predictive distribution describes the law governing future observations given the past. When this sequence is exchangeable, de Finetti’s representation theorem (see 1, 14, 16, 17 for classical results and 6 for modern information–theoretic extensions) shows that prediction amounts to averaging over i.i.d. laws drawn from a latent measure. Our goal is to understand how this predictive law behaves when the underlying sequence is subject to constraints—when moment conditions, partial identification, or structural symmetries restrict the admissible laws.

We study the *concentration* of the Bayesian predictive distribution toward a single law determined by the geometry of these constraints. We refer to this phenomenon as *predictive collapse*: partial information causes predictive uncertainty to contract at a rate governed by curvature. The paper develops a finite, curvature–adaptive framework that explains this contraction directly, without appealing to asymptotic or large–deviation limits, thereby extending the logic of Bayesian coherence to the geometry of constrained prediction.

## 1.1 Connections with Prior Work

Our approach builds on the literature on partial-information models and constrained inference, including empirical likelihood [49, 50], exponentially tilted likelihood [54], and proper Bayesian likelihoods [45]. Following the information-theoretic program of Jaynes [28], Bayesian updating under constraints is interpreted as an *information projection* onto the space of admissible laws. This connects to the Heath–Sudderth representation [24], where prediction arises from a discrete prior supported on admissible empirical measures. Classical formulations, empirical likelihood (EL; 49), Bayesian empirical likelihood (BEL; 55), and Bayesian exponentially tilted empirical likelihood (BETEL; 11), correspond to alternative choices of this prior geometry. Our analysis provides the unifying curvature-based principle governing their finite-sample contraction behavior.

From a probabilistic standpoint, the framework extends the tradition inaugurated by Bruno de Finetti. In his foundational papers [14], de Finetti established that exchangeability implies the existence of a directing measure for predictive distributions. Heath and Sudderth [24] formalized this representation in finite form, and subsequent developments by Diaconis, Freedman, and Aldous [1, 16, 17] linked it to Bayesian nonparametrics and empirical-process theory. More recently, Berta et al. [6] derived a finite de Finetti bound via information-theoretic methods, further enriching this line of work. Our construction adapts these ideas to *constrained exchangeable sequences*, where moment restrictions act as geometric deformations of the directing measure and predictive curvature replaces Fisher information as the local measure of learning strength.

Finally, this geometric view unites the large-deviation and martingale perspectives of Sanov and Doob. Doob [18] interpreted posterior convergence as a martingale property, while Sanov’s theorem [53] characterized empirical-measure concentration through information divergence. Recent

work by Polson and Zantedeschi [51] synthesized these strands through parameter emergence in exchangeable experiments; we extend their analysis to the dual phenomenon of predictive *collapse*, deriving finite-sample, curvature-controlled bounds on the contraction of uncertainty.

## 1.2 Contributions

*On the theoretical side.* We work throughout with a finite sample space  $\mathcal{X} = \{1, \dots, k\}$  and identify each probability distribution  $P$  on  $\mathcal{X}$  with its probability vector  $(P(1), \dots, P(k))$  in the simplex  $\Delta_k$ . Given moment constraints  $\mathbb{E}_P[h(X)] = \alpha$ , we write  $P^*$  for the information projection (KL-minimizer) of a baseline law  $Q$  onto the constraint set,  $H^*$  for the Hessian of the KL divergence restricted to the tangent space of the constraint manifold at  $P^*$ , and  $\lambda_\theta$  for the Lagrange multiplier enforcing the constraints. Precise definitions appear in Section 2.

We derive a finite-sample analogue of local asymptotic normality (LAN) in the sense of Le Cam and Hájek [39, 41], specialized to constrained exchangeable sequences. Starting from the tilted de Finetti representation,

$$\mathcal{L}(X_{1:m} \mid P_n \in E_n) = \int P^{\otimes m} \pi_n(dP \mid E_n),$$

Theorem 3.1 (*Gaussian de Finetti*) shows that conditioning on empirical moment restrictions induces an exponential tilt on the directing measure,

$$\pi_n(dP \mid E_n) \approx \exp\left\{-\frac{n}{2}(P - P^*)^\top H^*(P - P^*)\right\} dP,$$

whose local expansion yields a Gaussian weighting on the tangent space of the constraint manifold. Corollary 4.1 (*Finite LAN Limit*) identifies the curvature of this weighting with the information-geometric Hessian  $H^*$ , providing a discrete predictive analogue of the Fisher information in the LAN experiment. This reproduces, in finite form, the local quadratic expansion underlying the Le Cam-Hájek theory and suggests *predictive collapse* as the finite counterpart of asymptotic contiguity. Building on these results, Theorem 5.1 (*BETEL as Conditional Likelihood*) shows that the Bayesian exponentially tilted empirical likelihood arises as the conditional likelihood implied by exchangeability and moment constraints:

$$\pi(\theta \mid X_{1:n}) \propto \pi(\theta) \prod_{i=1}^n P_\theta^*(X_i),$$

where the exponential tilt  $\exp\{\lambda_\theta^\top h(x)\}$  is absorbed into  $P_\theta^*$ . Together, these results demonstrate that curvature—rather than parametrization—governs the rate and stability of predictive contraction, providing the theoretical foundation for all subsequent methodological results.

*On the methodological side.* Our framework extends these theoretical results to unify and reinterpret classical inferential procedures through their implied curvature geometry. It clarifies how empirical likelihood (EL), Bayesian empirical likelihood (BEL), exponentially tilted empirical likelihood (ETEL and BETEL), generalized method of moments (GMM), and generalized estimating equations (GEE) arise as specializations of the same conditional predictive law. Theorem 5.3 (*Quadratic Expansion of the Conditional Likelihood*) shows that GMM represents the optimal quadratic approximation to BETEL in the LAN limit,

$$\mathcal{L}_{\text{cond}}(\theta) \approx \exp\left[-\frac{n}{2} \bar{g}_n(\theta)^\top (A_\theta H_\theta^{*-1} A_\theta^\top)^{-1} \bar{g}_n(\theta)\right],$$

while Theorem 5.4 (*Curvature–Robust Estimating Equations*) demonstrates that GEE inherits its robustness from effective curvature adjustments within the tangent space. Finally, Theorem 6.1 (*Predictive Misspecification*) extends the analysis to model misspecification via Berk’s theorem [5], showing that curvature determines both posterior concentration rates and the brittleness of inference under approximate constraints. Together, these results provide a single predictive geometry that unifies large-deviation, empirical-likelihood, and Bayesian approaches.

*On the practical side.* The curvature–based representation offers a quantitative diagnostic for identification strength and model robustness. Computing  $\lambda_{\min}(H^*)$  directly reveals whether moment conditions are strongly or weakly identifying: small values indicate flat geometry, slow learning, and robustness; large values correspond to sharp curvature, rapid concentration, and potential brittleness. The same parameter guides calibration of empirical-likelihood weights, moment penalties in GMM, and tempered posteriors. Sample–size requirements scale as

$$n \gtrsim \frac{m^2 \log(1/\varepsilon)}{\varepsilon^2 \lambda_{\min}(H^*)}$$

to achieve predictive precision  $\varepsilon$ , providing concrete guidance for experimental design. Together, these insights position predictive collapse as a unifying principle for constrained statistical inference and a practical tool for uncertainty quantification under partial information.

*Scope and conventions.* The results of this paper are established rigorously for finite sample spaces  $\mathcal{X} = \{1, \dots, k\}$  under exchangeability and affine moment constraints. Within this setting, Theorems 3.1 and 3.4 provide non-asymptotic bounds with explicit dependence on the curvature parameter  $\lambda_{\min}(H^*)$ . The connections to BETEL, GMM, GEE, and Berk’s theorem (Theorems 5.1–6.1) are derived via local quadratic approximation and hold to leading order in the LAN regime. The broader geometric interpretations—linking predictive collapse to Le Cam theory, information geometry, and large-deviation principles—are offered as a unifying perspective rather than as standalone theorems; they are supported by the formal results but are not claimed to extend beyond the finite, exchangeable setting without additional work.

Figure 1 provides an illustration of the steps taken in the paper to obtain our results.

## 2 Bayesian Prediction Under Constraints

We consider predictive inference for discrete observations under moment constraints, a framework broad enough to capture many practical problems, yet structured enough to allow precise geometric analysis. The setting is deliberately finite to highlight geometric mechanisms rather than measure-theoretic complexity.

Let  $\mathcal{X} = \{1, \dots, k\}$  be a finite sample space with  $k \geq 2$  elements. We observe an exchangeable sequence

$$X_1, \dots, X_n, \quad P_n = \frac{1}{n} \sum_{i=1}^n \delta_{X_i},$$

where  $P_n$  is the empirical measure. Let  $Q$  be a *baseline* (reference) distribution on  $\mathcal{X}$  satisfying  $Q(x) > 0$  for all  $x$ . When the data-generating law coincides with  $Q$ , the setting is well-specified; when it does not, the framework reduces to the misspecified analysis of Section 6, with  $Q$  serving as the anchor for the KL projection. Throughout, we identify each probability distribution  $P$

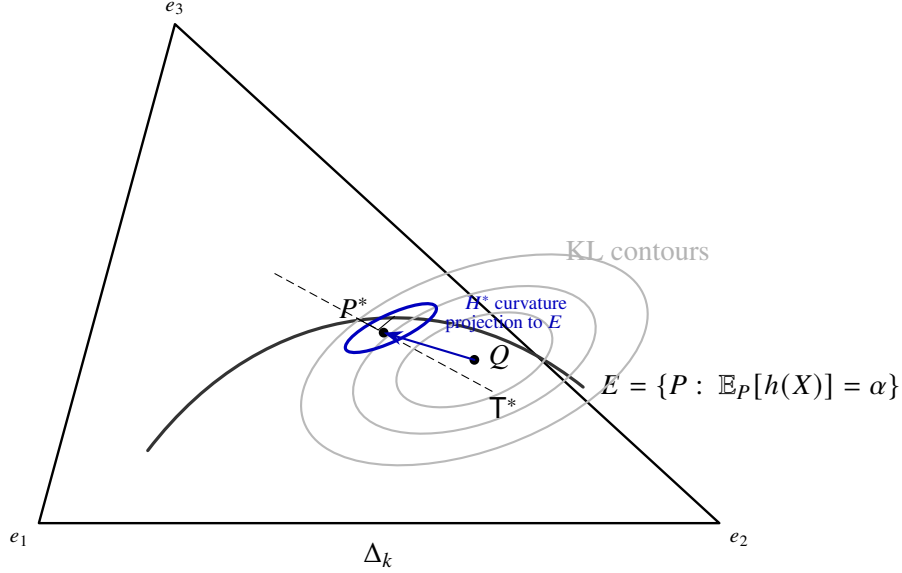


Figure 1: Constraint geometry inside the probability simplex  $\Delta_k$ , adapted from the information–geometric visualizations of Kass [30], Kass and Vos [31]. The feasible manifold  $E$  represents the distributions satisfying  $\mathbb{E}_P[h(X)] = \alpha$ . The information projection  $P^*$  is where a Kullback–Leibler contour centered at the baseline model  $Q$  is tangent to  $E$ . The tangent space  $\mathbb{T}^*$  and the local curvature encoded by the projected Hessian  $H^*$  govern the Gaussian weighting in Theorem 3.1, quantifying predictive contraction via  $\lambda_{\min}(H^*)$ .

on  $\mathcal{X}$  with its probability vector  $(P(1), \dots, P(k)) \in \mathbb{R}^k$ ; all vector operations on  $P$  are to be understood in this sense. Although discrete, this formulation encompasses numerous applications: categorical surveys, multinomial outcomes in clinical trials, finite partitions in nonparametric Bayes, or discretizations of continuous phenomena. While our development proceeds in a finite, exchangeable setting, approximate and finite de Finetti representations justify this reduction and quantify errors; see Aldous [1], Diaconis and Freedman [16, 17].

Moment constraints arise naturally across domains. In survey analysis, expected ratings may be fixed by design; in portfolio theory, risk limits constrain volatility; in quality control, proportions of defect types must match specifications; and in text analysis, topic proportions obey similarity bounds. Such restrictions define an affine manifold of feasible laws, within which prediction must operate.

## 2.1 Constraint Structure and Geometry

Let  $h : \mathcal{X} \rightarrow \mathbb{R}^d$  be a bounded feature map with  $\|h\|_\infty \leq B < \infty$ , and let  $\alpha \in \mathbb{R}^d$  specify the target moments. The feasible set of probability distributions is

$$E = \left\{ P \in \Delta_k^\circ : \mathbb{E}_P[h(X)] = \alpha \right\}, \quad \Delta_k^\circ = \left\{ p \in \mathbb{R}_+^k : \sum_{i=1}^k p_i = 1, p_i > 0 \right\}.$$

Writing  $A = [h(1) \ \dots \ h(k)] \in \mathbb{R}^{d \times k}$ , we may express the feasible set as the intersection

$$E = \{ P \in \Delta_k^\circ : AP = \alpha \}.$$

When  $A$  has rank  $d < k - 1$  and  $\alpha$  lies in the convex hull of  $\{h(x) : x \in \mathcal{X}\}$ ,  $E$  forms a smooth  $(k - 1 - d)$ -dimensional submanifold of the simplex. Most constraints of practical interest—means, variances, correlations, or inequalities handled via slack variables—are affine or reducible to affine form, making this geometry broad yet analytically tractable.

*Information projection.* Given a baseline model  $Q$ , the *information projection* onto  $E$  is defined by

$$P^* = \arg \min_{P \in E} D_D(P \| Q), \quad D_D(P \| Q) = \sum_{x \in \mathcal{X}} P(x) \log \frac{P(x)}{Q(x)}.$$

The point  $P^*$  balances fidelity to  $Q$  with adherence to the constraints and serves as the deterministic benchmark for prediction. Its local curvature will determine the rate and shape of finite-sample contraction.

*Tangent space and projected Hessian.* Because  $\sum_x P(x) = 1$ , feasible perturbations around  $P^*$  lie in the tangent space

$$\mathbb{T}^* = \{v \in \mathbb{R}^k : \mathbf{1}^\top v = 0, Av = 0\},$$

of dimension  $r = k - 1 - d$ . On this subspace, the ambient Hessian of the Kullback–Leibler divergence,  $\nabla^2 D_D(P \| Q) = \text{diag}(1/P)$ , is projected to yield the effective curvature operator

$$H^* = \Pi_{\mathbb{T}^*} \text{diag}\left(\frac{1}{P^*}\right) \Pi_{\mathbb{T}^*},$$

where  $\Pi_{\mathbb{T}^*}$  denotes the orthogonal projection onto  $\mathbb{T}^*$ . If  $V$  is an orthonormal basis for  $\mathbb{T}^*$ , then

$$H^* = V^\top \text{diag}\left(\frac{1}{P^*}\right) V.$$

This operator represents the Fisher–Rao metric restricted to the constraint manifold [48] and functions as the local *information curvature tensor* of  $E$  at  $P^*$ . From a convex–analytic viewpoint, this corresponds to the I-divergence projection of Csizsár [13]; from the differential–geometric view, it coincides with the dual affine connection of information geometry [2, 3]. Together these perspectives justify interpreting  $H^*$  as the fundamental local operator governing predictive contraction.

*Curvature interpretation.* The smallest eigenvalue  $\lambda_{\min}(H^*)$  quantifies *constraint curvature*. Large  $\lambda_{\min}(H^*)$  implies sharp curvature, strong identification, and rapid predictive concentration, whereas small  $\lambda_{\min}(H^*)$  corresponds to flatter geometry, weaker identification, and slower contraction. This curvature constant will appear throughout the paper as the single geometric parameter linking constraint structure and predictive learning.

## 2.2 Predictive Representation

Let  $\mathcal{X}$  be a finite observation space, and let  $\mathcal{P}$  denote the simplex of all probability measures on  $\mathcal{X}$ . For each sample size  $n$ , let  $\mathcal{P}_n \subset \mathcal{P}$  denote the set of empirical (type) distributions supported on at most  $n$  points, and let  $E = \{P \in \mathcal{P} : \mathbb{E}_P[h(X)] = \alpha\}$  be the population constraint manifold induced by a bounded feature map  $h : \mathcal{X} \rightarrow \mathbb{R}^d$  and target moment  $\alpha \in \mathbb{R}^d$ . The feasible empirical types are then  $E_n = E \cap \mathcal{P}_n$ .

We observe  $X_{1:n} = (X_1, \dots, X_n)$  and denote by  $P_n$  its empirical distribution. The goal is to predict  $m = o(n)$  future observations  $X_{n+1}, \dots, X_{n+m}$  under the conditioning event that the past sample satisfies the constraint  $P_n \in E_n$ . The corresponding Bayesian predictive law is therefore

$$\mu_{n,m} = \mathcal{L}(X_{n+1:n+m} \mid P_n \in E_n).$$

By the Heath–Sudderth finite representation [24],

$$\mu_{n,m}(x_{1:m}) = \sum_{P \in E_n} \Pr(X_{1:m} = x_{1:m} \mid P_n = P) \Pr(P_n = P \mid P_n \in E_n),$$

where the first factor is the hypergeometric sampling probability of drawing  $m$  observations without replacement from the empirical type  $P$ , and the second factor gives the conditional weight of each feasible empirical distribution.

The central question is how close the constrained predictive law  $\mu_{n,m}$  is to the benchmark product measure  $(P^*)^{\otimes m}$ , where  $P^*$  denotes the *information projection* of the unconstrained law  $Q$  onto  $E$ , defined as

$$P^* = \arg \min_{P \in E} D_D(P \parallel Q).$$

The analysis to follow shows that this proximity is governed by the curvature parameter  $\lambda_{\min}(H^*)$ , the smallest eigenvalue of the information–geometric Hessian

$$H^* = \Pi_{\mathbb{T}^*} \nabla^2 D_D(P \parallel Q) \Big|_{P=P^*} \Pi_{\mathbb{T}^*},$$

the Hessian of the KL divergence projected onto the tangent space  $\mathbb{T}^*$  of the constraint manifold at  $P^*$  (see Section 2.1 for the precise definition). This curvature quantifies the local sharpness of the constraint manifold and thus determines the rate of predictive collapse.

### 3 Main Results

Predictive collapse arises because, once structural constraints are imposed, the posterior predictive distribution places nearly all its probability on empirical types close to the information projection  $P^*$ . The rate of this concentration is determined by  $\lambda_{\min}(H^*)$ : large curvature implies fast concentration, while flat geometry yields slower learning and greater robustness.

#### 3.1 Geometric Mechanism

The Heath–Sudderth representation expresses the constrained predictive law as a mixture over feasible empirical types  $P \in E_n$ , weighted by their multinomial likelihoods. Expanding the Kullback–Leibler divergence around  $P^*$  gives

$$D_D(P \parallel Q) = D_D(P^* \parallel Q) + \frac{1}{2}(P - P^*)^\top H^*(P - P^*) + O(\|P - P^*\|_2^3),$$

so that, to second order, the weights behave like a Gaussian density on the tangent space  $\mathbb{T}^* = \{v \in \mathbb{R}^k : \mathbf{1}^\top v = 0, Av = 0\}$  with precision matrix  $nH^*$ . Empirical types farther than order  $n^{-1/2}$  from  $P^*$  therefore have exponentially small probability.

#### 3.2 Curvature–Adaptive Localization

To control the discrete–continuous approximation error, we introduce a curvature–adaptive localization window around  $P^*$ ,

$$\rho_n = \left( \frac{2 \log n}{\lambda_{\min}(H^*)} \right)^{1/2}, \quad \mathcal{W}_n = \{P \in E_n : \|P - P^*\|_2 \leq \rho_n / \sqrt{n}\}.$$

The effective radius  $\rho_n/\sqrt{n}$  expands when the constraint manifold is flat (small  $\lambda_{\min}$ ) and contracts under strong curvature. This construction follows the localization method of Lanford [35, 36] for bridging discrete combinatorics and continuous Gaussian approximations, as further developed in the large-deviation analysis of Ellis [19]. Here it is applied to constrained exchangeable sequences. A formal operator-theoretic characterization, showing that  $\rho_n$  arises as a fixed point of a regularization operator, is provided in Appendix A.

### 3.3 Tilted Finite Gaussian de Finetti Theorem

Consequently,  $\mathcal{W}_n$  defines the smallest neighborhood in which both the Gaussian and lattice approximations hold uniformly, yielding a global  $O(n^{-1/2} \text{polylog } n)$  accuracy.

**Theorem 3.1** (Tilted Finite Gaussian de Finetti). *Let*

$$\phi_{H^*}(v) = |H^*|^{1/2} (2\pi)^{-r/2} \exp\left(-\frac{1}{2}v^\top H^* v\right)$$

denote the Gaussian density on the tangent space  $\mathbb{T}^*$ , where  $r = \dim(\mathbb{T}^*)$ . For any measurable set  $A \subset \mathcal{X}^m$  with  $m = O(n^\eta)$  for some fixed  $\eta < 1/2$ ,

$$\mu_{n,m}(A) = \int_{\mathbb{T}^*} P_{P(v)}^{\otimes m}(A) \phi_{H^*}(v) dv + E_n(A),$$

where  $P(v) = \Pi(P^* + n^{-1/2}v)$  is the local chart projection of  $P^* + n^{-1/2}v$  onto  $E$ , and the error term satisfies

$$|E_n(A)| \leq C_{\text{geo}} n^{-1/2} \text{polylog}(n),$$

for a constant  $C_{\text{geo}}$  depending only on  $(|\mathcal{X}|, d, p_{\min}^*)$  and the local curvature near  $P^*$ .

*Remark 3.2* (Interpretation). Conditioning on the constraints replaces the flat multinomial prior with a Gaussian measure on the manifold, centred at  $P^*$  with covariance  $(nH^*)^{-1}$ . Predictive collapse is therefore a geometric manifestation of curvature: steep curvature compresses the Gaussian, whereas flat curvature leaves it diffuse. The result provides a finite, curvature-adaptive analogue of de Finetti's representation for exchangeable sequences.

*Remark 3.3* (Tilted Finite de Finetti). The mixture in Theorem 3.1 is not uniform over empirical types but *exponentially tilted* around the information projection  $P^*$ . The quadratic form  $v^\top H^* v$  encodes the curvature of the constraint manifold, so the resulting representation is a *tilted finite de Finetti theorem*: exchangeability holds, but the prior over empirical laws is reweighted by the constraint-induced information curvature. This tilt unifies the de Finetti mixture with exponential weighting, providing the finite predictive counterpart to large-deviation geometry.

### 3.4 Curvature and Predictive Contraction

The Gaussian approximation of Theorem 3.1 implies that deviations of the constrained predictive law  $\mu_{n,m}$  from its deterministic limit  $(P^*)^{\otimes m}$  arise from three finite-sample effects. The first is the *hypergeometric correction* due to sampling without replacement, contributing a term of order  $O\{m^2/(np_{\min}^*)\}$ , where  $p_{\min}^* = \min_x P^*(x)$ . The second is the *local deviation* within the Lanford window  $\mathcal{W}_n = \{P : \|P - P^*\| \leq \rho_n/\sqrt{n}\}$ , controlled by the Lipschitz continuity of the likelihood

and scaling as  $O(m \rho_n / \sqrt{n})$ . The third is the exponentially small *tail mass* outside the window, of order  $\exp\{-\frac{1}{2} \lambda_{\min}(H^*) \rho_n^2\} = n^{-1}$ . Balancing the first two effects yields the curvature–adaptive choice

$$\rho_n^2 = \frac{2 \log n}{\lambda_{\min}(H^*)}.$$

**Theorem 3.4** (Predictive collapse). *Assume the conditions of Theorem 3.1 and let  $m = o(\sqrt{n \lambda_{\min}(H^*) / \log n})$ . Then*

$$\|\mu_{n,m} - (P^*)^{\otimes m}\|_{\text{TV}} \leq C_{\text{geo}} m \sqrt{\frac{\log n}{n \lambda_{\min}(H^*)}} + C'_{\text{geo}} \frac{m^2}{n p_{\min}^*} + o(n^{-1/2}),$$

where  $C_{\text{geo}}$  and  $C'_{\text{geo}}$  depend only on  $(|\mathcal{X}|, d, p_{\min}^*)$  and on the local curvature of the constraint manifold near  $P^*$ .

*Remark 3.5* (Interpretation). The leading term represents *geometric contraction*: predictive uncertainty shrinks at rate  $O((n \lambda_{\min}(H^*))^{-1/2})$ , governed by the curvature radius of the constraint manifold. The second term is the finite–population correction, negligible whenever  $m \ll \sqrt{n}$ . Hence increasing curvature or enlarging the sample size forces the predictive law to *collapse* sharply onto the information projection  $P^*$ .

### 3.5 Computation of the Curvature

The curvature parameter  $\lambda_{\min}(H^*)$  can be obtained by a straightforward sequence of convex and linear-algebraic computations. First, the information projection  $P^*$  is determined by solving the convex optimization problem

$$P^* = \arg \min_{AP=\alpha} \sum_x P(x) \log \frac{P(x)}{Q(x)},$$

which enforces the affine moment constraints while preserving normalization. Given this optimum, one constructs a basis  $V$  for the tangent space

$$\mathbb{T}^* = \{v : \mathbf{1}^\top v = 0, Av = 0\},$$

representing feasible first-order perturbations around  $P^*$ . The local curvature matrix is then obtained as

$$H^* = V^\top \text{diag}(1/P^*)V,$$

and its smallest eigenvalue  $\lambda_{\min}(H^*)$  provides the effective curvature of the constraint manifold.

For standard moment constraints,  $\lambda_{\min}(H^*)$  typically lies between  $(p_{\max}^*)^{-1}$  and  $(p_{\min}^*)^{-1}$ , with sharper bounds achievable when the constraint matrix  $A$  is aligned with coordinate axes. In practice, this computation is numerically stable even for moderate dimensions, since  $H^*$  is positive definite on the reduced tangent space and inherits the conditioning of the moment Jacobian  $A$ .

### 3.6 Interpretation and Implications

The two theorems together give a unified geometric picture of constrained prediction. The discrete Gaussian approximation shows that the constrained posterior predictive behaves like a normal distribution on the manifold  $E$  with precision proportional to curvature. The predictive-collapse bound translates this geometry into rates: the stronger the curvature, the faster the predictive uncertainty vanishes. Flat constraint surfaces lead to slow learning and wide predictive spread, while curved surfaces, corresponding to strongly informative or tightly binding constraints, produce rapid convergence to a single predictive law. Thus, curvature acts as an intrinsic measure of statistical rigidity, determining how quickly exchangeable prediction under constraints transitions from probabilistic to deterministic behavior.

## 4 Asymptotic and Geometric Connections

The discrete Gaussian approximation developed above implies that constrained predictive laws satisfy a local asymptotic normality property analogous to that of parametric experiments. In the limit, the entire predictive mechanism behaves as a curved exponential family centred at the information projection  $P^*$ . This identification aligns with the differential-geometric structure of exponential families formalized by Brown [9] and connects to the asymptotic theory of statistical experiments initiated by Le Cam [39] and its modern expositions by Le Cam and Yang [40], van der Vaart [58], in which local asymptotic normality (LAN) provides the bridge between finite models and their Gaussian tangent experiments.

**Corollary 4.1** (Local asymptotic normality). *Under the conditions of Theorem 3.1, let  $\Delta_n = \sqrt{n}(P_n - P^*)$  and let  $\xi_m$  denote the Gaussian shift induced by the tangent coordinates of the predictive experiment. Then, uniformly over bounded sequences of alternatives,*

$$\log \frac{d\mu_{n,m}}{d(P^*)^{\otimes m}}(X_{n+1:n+m}) = \Delta_n^\top \xi_m - \frac{1}{2} \Delta_n^\top H^* \Delta_n + o_p(1).$$

*Hence the sequence of predictive experiments  $\{\mu_{n,m}\}_n$  is contiguous to the exponential-tilt family at parameter  $\theta^*$  corresponding to  $P^*$ , with Fisher information matrix  $H^*$ .*

**Remark 4.2** (Connection with Le Cam’s theory). The LAN expansion in Corollary 4.1 identifies the constrained predictive mechanism with a Gaussian shift experiment on the tangent space  $(T^*, H^*)$ . In Le Cam’s metric for statistical experiments, this means that the sequence  $\{\mu_{n,m}\}$  converges to a limit experiment given by observation of a Gaussian random element with covariance  $(H^*)^{-1}$ . The predictive collapse phenomenon therefore admits a coordinate-free formulation: it is precisely the convergence of predictive experiments to their Gaussian tangent model, with curvature determining the information content of the limit.

**Remark 4.3** (Coordinate invariance). The quantities appearing in our bounds are invariant under smooth reparameterizations of the constraint manifold. The matrix  $H^*$  is the restriction of the Riemannian information metric to  $T^*$ , and  $\lambda_{\min}(H^*)$  depends only on the intrinsic geometry of  $E$ , not on its coordinate representation. Thus the results describe geometric, not coordinate-features of predictive concentration.

## 4.1 Practical Implications

Although developed in a geometric–asymptotic setting, the results carry direct implications for model design, diagnostics, and uncertainty assessment. The curvature matrix  $H^*$  determines how efficiently information is translated into predictive accuracy. Well-conditioned constraints—for instance, moment conditions defined by nearly orthogonal rather than collinear features, yield larger  $\lambda_{\min}(H^*)$  and therefore faster convergence of the predictive distribution. This parameter serves as a quantitative measure of identifiability: small values of  $\lambda_{\min}(H^*)$  indicate weak curvature and a flat constraint geometry, conditions under which predictive collapse can be slow or unstable.

The sample size required to achieve a given predictive precision follows the scaling

$$n \gtrsim \frac{m^2 \log(1/\epsilon)}{\epsilon^2 \lambda_{\min}(H^*)},$$

which formalizes the intuitive trade-off between curvature, data volume, and prediction horizon. Greater curvature lowers the data demand for a fixed total-variation error  $\epsilon$ , while weaker curvature necessitates larger samples to attain the same accuracy. In practice, computing  $\lambda_{\min}(H^*)$  provides a simple diagnostic of constraint strength and geometric conditioning.

The same curvature parameter also governs the construction of predictive confidence regions. Rather than relying solely on point forecasts, one may report the range of predictive distributions lying within total-variation distance

$$C_{\text{geo}} m \sqrt{\frac{\log n}{n \lambda_{\min}(H^*)}}$$

of the limiting law  $(P^*)^{\otimes m}$ . Such regions reflect the intrinsic geometry of constrained inference and offer a principled form of uncertainty quantification.

Viewed through this lens, predictive collapse fits naturally within Le Cam’s coordinate-free asymptotic theory. The curvature matrix  $H^*$  plays the role of Fisher information, determining both the rate of contraction and the local geometry of the limiting Gaussian experiment. Constrained prediction thus emerges not as a finite-sample correction, but as a manifestation of a universal asymptotic geometry: as information accumulates, predictive distributions evolve along geodesics of the information metric, collapsing onto the manifold point  $P^*$  at a curvature-controlled rate.

## 5 Connections with Exponentially Tilted Empirical Likelihood

Exponentially tilted empirical likelihood (ETEL) and its Bayesian analogue (BETEL) have achieved notable success in semiparametric inference [27, 32, 37, 38, 52, 55]. Yet their theoretical justification is often presented as a pragmatic extension of empirical likelihood rather than as a direct consequence of probabilistic first principles. Our framework derives ETEL and BETEL from such principles, showing that they emerge naturally as conditional likelihoods under exchangeability and moment constraints. In particular, BETEL coincides with the *conditional likelihood in the limit experiment* defined by the curvature of the constraint manifold, thus linking de Finetti coherence with information-geometric inference.

Let the moment constraints be  $\mathbb{E}_P[h(X)] = \alpha(\theta)$  for  $\theta \in \Theta \subset \mathbb{R}^p$ , and define

$$E_\theta = \{P \in \Delta_k^\circ : \mathbb{E}_P[h(X)] = \alpha(\theta)\}, \quad P_\theta^* = \arg \min_{P \in E_\theta} D_D(P \| Q).$$

The information projection takes the exponential form

$$P_\theta^*(x) = Q(x) \exp\{\lambda_\theta^\top h(x)\} / Z(\lambda_\theta),$$

with  $\lambda_\theta$  chosen to enforce  $\mathbb{E}_{P_\theta^*}[h] = \alpha(\theta)$ . This recovers the exponential tilt underlying Qin and Lawless [52] and Newey and Smith [47].

**Theorem 5.1** (BETEL as conditional likelihood). *Under standard smoothness and interiority conditions, the conditional law of the empirical type given the constraint,*

$$\Pr(P_n \in \cdot \mid P_n \in E_{\theta,n}), \quad E_{\theta,n} = E_\theta \cap \mathcal{P}_n,$$

*induces, up to asymptotically smooth Jacobian factors, the BETEL posterior*

$$\pi(\theta \mid X_{1:n}) \propto \pi(\theta) \prod_{i=1}^n P_\theta^*(X_i) (1 + o_p(1)),$$

*where  $P_\theta^*(x) = Q(x) \exp\{\lambda_\theta^\top h(x)\} / Z(\lambda_\theta)$  already incorporates the exponential tilt. Hence BETEL coincides with the conditional likelihood implied by exchangeability and moment constraints in the LAN limit experiment.*

The proof follows from Theorem 3.1: conditioning on  $P_n \in E_{\theta,n}$  confines empirical types to a Gaussian neighborhood of  $P_\theta^*$ , and Lagrange duality converts this weighting into the exponential tilt. This geometric interpretation explains several known properties. First, semiparametric efficiency arises because  $P_\theta^*$  minimizes Kullback–Leibler divergence, so its Hessian  $H_\theta^*$  provides the semiparametric information bound. Second, the Bernstein–von Mises behavior established by Chib et al. [11, 12] follows from the discrete Gaussian law: the BETEL posterior is asymptotically normal with covariance  $H_{\theta_0}^{*-1}$ . Third, over-identification robustness emerges naturally because additional valid moments enlarge curvature, increasing  $\lambda_{\min}(H_\theta^*)$  and hence accelerating contraction.

**Corollary 5.2** (Posterior concentration). *For any prior with positive continuous density near  $\theta_0$ ,*

$$\Pr\left(\|\theta - \theta_0\|_2 > C \sqrt{\frac{\log n}{n \lambda_{\min}(H_{\theta_0}^*)}} \mid X_{1:n}\right) = O(n^{-c})$$

*for all  $c > 0$ . Moreover, the predictive law satisfies*

$$\|\mu_{n,m}^{\text{BETEL}} - (P_{\theta_0}^*)^{\otimes m}\|_{\text{TV}} = O\left(m \sqrt{\frac{\log n}{n \lambda_{\min}(H_{\theta_0}^*)}}\right).$$

Thus BETEL inherits both its efficiency and its rates directly from the constraint manifold’s curvature, situating it naturally within the geometry of moment-restricted inference.

## 5.1 GMM and GEE as Quadratic Approximations

While BETEL provides the exact conditional likelihood, computational considerations often favor quadratic approximations. We show that generalized method of moments (GMM; 23) and generalized estimating equations (GEE; 43) arise naturally as optimal second-order expansions of this likelihood, with their properties governed by the same curvature parameter. This connection situates our framework within the broader theory of moment-based estimation and quasi-likelihood, linking the geometric weighting implied by  $H^*$  to classical results on optimal GMM weighting and efficiency [26, 46, 59]. The curvature perspective thus provides a unified explanation for both efficiency under correct specification and robustness under model misspecification.

Let  $\bar{g}_n(\theta) = n^{-1} \sum_{i=1}^n g(X_i, \theta)$  be the sample moment residuals and  $A_\theta = \partial_\theta \mathbb{E}[g(X, \theta)]$  the moment Jacobian. The discrete Gaussian approximation implies that likelihood ratios on the manifold are governed by quadratic energy in the information metric  $H_\theta^*$ .

**Theorem 5.3** (GMM optimality). *The second-order expansion of the conditional log-likelihood is*

$$-\log \mathcal{L}_{\text{cond}}(\theta) = \frac{n}{2} \bar{g}_n(\theta)^\top W_\theta^{\text{opt}} \bar{g}_n(\theta) + O_p(n^{-1/2}),$$

where the optimal weight matrix

$$W_\theta^{\text{opt}} = \left[ (A_\theta|_{\mathbb{T}_\theta^*}) H_\theta^{*-1} (A_\theta|_{\mathbb{T}_\theta^*})^\top \right]^{-1}$$

is the inverse of the pushforward of the information metric through the moment map restricted to the tangent space.

This identifies the celebrated "optimal" GMM weight as pure geometry: it is the Riemannian metric induced on moment space by the information metric on the manifold. Semiparametric efficiency follows immediately in just-identified models, while over-identification improves rates by increasing  $\lambda_{\min}(H_\theta^*)$ .

For clustered outcomes with mean  $\mu_i(\theta)$ , Jacobian  $D_i(\theta)$ , and working covariance  $W_i(\theta)$ , the GEE estimating equation  $\sum_i D_i^\top W_i (Y_i - \mu_i) = 0$  corresponds to a quadratic loss with effective curvature

$$J(\theta) = \mathbb{E}[D_i(\theta)^\top W_i(\theta) D_i(\theta)].$$

**Theorem 5.4** (GEE robustness). *If  $\theta_0$  solves the population estimating equation and  $\lambda_{\min}(J(\theta_0)) > 0$ , then any consistent root  $\hat{\theta}$  satisfies*

$$\|\hat{\theta} - \theta_0\| = O_p\left(\sqrt{\frac{\log n}{n \lambda_{\min}(J(\theta_0))}}\right).$$

*If the working and true metrics are comparable,  $aH_{\theta_0}^* \preceq J(\theta_0) \preceq bH_{\theta_0}^*$ , then the rate is preserved up to factor  $a^{-1/2}$ , with asymptotic variance*

$$\sqrt{n}(\hat{\theta} - \theta_0) \xrightarrow{d} \mathcal{N}(0, J(\theta_0)^{-1} K(\theta_0) J(\theta_0)^{-1}),$$

where  $K(\theta) = \mathbb{E}[D_i^\top W_i \Sigma_i W_i D_i]$  is the Godambe sandwich middle [20, 21].

Thus GEE achieves robustness by replacing the exact information metric with a working approximation. Independence working correlations preserve rates whenever true correlations are moderate, while pathological choices that nearly annihilate directions in  $\text{span}(D_i)$  destroy stability by driving  $\lambda_{\min}(J)$  to zero.

## 5.2 Unified perspective

The geometric framework reveals a hierarchy of approximations to the constraint manifold’s conditional likelihood. BETEL provides exact conditional inference, GMM gives its optimal quadratic approximation, and GEE trades efficiency for robustness through working metrics. All three methods are governed by the same curvature principle. Strong curvature, characterized by large  $\lambda_{\min}(H^*)$ , produces fast convergence and narrow confidence regions but potential brittleness under misspecification. Weak curvature, with small  $\lambda_{\min}(H^*)$ , yields slow convergence and wide regions but greater robustness. GEE achieves an intermediate position through its effective curvature  $J(\theta)$ , gaining robustness via metric approximation at the cost of sandwich variance inflation. This unifies efficiency, identification, and misspecification as different facets of constraint geometry, with practical diagnostics available through computing or bounding  $\lambda_{\min}(H^*)$  at fitted solutions.

## 6 Misspecification, Berk’s theorem, and geometric tempering

Berk’s classical result [5] is often viewed as a pathology: under model misspecification, the posterior concentrates at the wrong parameter. Geometrically, however, it represents the limiting case of constrained inference when the truth lies outside the constraint set. If  $P_0 \in E$ , the information projection coincides with the truth ( $P^* = P_0$ ) and predictive or posterior collapse occurs at a curvature-controlled rate. If  $P_0 \notin E$ , the same mechanism governs contraction toward the pseudo-true projection

$$P^* = \arg \min_{P \in E} D_D(P \| P_0),$$

so misspecification alters only the target, not the dynamics of convergence. This geometric interpretation parallels modern analyses of misspecified posteriors in the Bernstein–von Mises framework [34] and in generalized Bayesian inference [7, 22, 25, 56], where curvature plays the role of local information content governing both contraction rate and robustness. Within our formulation, the discrete Gaussian weighting and the minimal eigenvalue  $\lambda_{\min}(H^*)$  jointly determine the speed and stability of learning under misspecification.

### 6.1 Berk’s Theorem via Constraint Curvature

Let  $\theta_0$  minimize  $D_D(P_0 \| P_\theta)$  over  $\theta \in \Theta$  and write  $H_{\theta_0}^*$  for the information-metric Hessian on the manifold at  $\theta_0$ . The inverse Sanov approximation yields finite-sample control that complements the classical large-sample statement.

**Theorem 6.1** (Berk’s theorem via curvature). *Assume standard smoothness/interiority, bounded moments, and a prior with positive continuous density near  $\theta_0$ . Then, for some constants  $c, C > 0$  depending on local geometry and the prior,*

$$\Pr\left(\|\theta - \theta_0\|_2 > \varepsilon \mid X_{1:n}\right) \leq C \exp\left\{-c n \lambda_{\min}(H_{\theta_0}^*) \varepsilon^2\right\},$$

and hence

$$\|\theta - \theta_0\|_2 = O_p\left(\sqrt{\frac{\log n}{n \lambda_{\min}(H_{\theta_0}^*)}}\right).$$

This refines the misspecified Bernstein–von Mises picture [e.g. 33]: curvature dictates the local information content and the rate at which the posterior contracts around the pseudo-true parameter. Large curvature accelerates learning yet increases brittleness under model error; small curvature slows learning but yields thicker, more robust posteriors. The same phenomenon holds predictively.

**Corollary 6.2** (Predictive misspecification). *For  $m = o(\sqrt{n \lambda_{\min}(H_{\theta_0}^*)/\log n})$ ,*

$$\|\mu_{n,m} - (P_{\theta_0}^*)^{\otimes m}\|_{\text{TV}} = O\left(m \sqrt{\frac{\log n}{n \lambda_{\min}(H_{\theta_0}^*)}}\right).$$

*Thus forecasts converge to the pseudo-true predictive law at the same curvature-controlled rate.*

Practically, the diagnostic is immediate: compute or bound  $\lambda_{\min}(H^*)$  at fitted solutions. Values near zero indicate flat geometry and resilience to misspecification at the cost of slower learning; large values indicate sharp geometry and speed, but potential overconfidence if the constraint is wrong. Monitoring how the fitted pseudo-true parameter stabilizes with  $n$ , and how  $\lambda_{\min}(H^*)$  evolves, gives an early-warning signal of brittleness.

## 6.2 Safe Bayes and Geometric Tempering

Tempering encompassing power posteriors, fractional Bayes, and Safe Bayes, rescales the log-likelihood by a factor  $1/T$  [7, 22, 25, 56], thereby dilating the information geometry of the posterior. In our setting, this corresponds to scaling the curvature matrix as  $H^* \mapsto H^*/T$ , so that the tempered posterior contracts at a rate governed by  $\lambda_{\min}(H^*/T)$ . In geometric terms, tempering simply rescales curvature: the tempered Hessian is  $H^*/T$ , and the predictive-collapse term becomes

$$m \sqrt{\frac{\log n}{n \lambda_{\min}(H^*/T)}} = m \sqrt{\frac{T \log n}{n \lambda_{\min}(H^*)}}.$$

Tempering therefore trades speed for robustness in a controlled, metric-level manner.

**Proposition 6.3** (Curvature-adaptive tempering). *Let  $\widehat{\lambda}_{\min}$  be a consistent local estimate of  $\lambda_{\min}(H^*)$ . Any choice  $T = T(\widehat{\lambda}_{\min})$  that keeps  $T/\widehat{\lambda}_{\min}$  bounded above and away from zero yields a collapse rate  $O(m\sqrt{\log n/n})$ , up to constants uniform over models with comparable curvature. In particular, setting*

$$T(\widehat{\lambda}_{\min}) = 1 + \beta \log(1 + \widehat{\lambda}_{\min}/\lambda_0), \quad \beta, \lambda_0 > 0,$$

*stabilizes rates across brittle and flat regimes while preserving nominal calibration asymptotically.*

Operationally, one estimates curvature at a preliminary fit, inflates  $T$  when geometry is sharp, and deflates it when geometry is flat. This regularizes misspecification without compromising coherence: tempering acts directly on the information metric rather than through ad hoc penalties. In practice, one may report both standard and curvature-adaptive tempered posteriors; discrepancies indicate either model tension or excessive brittleness. Because curvature governs both parameter and predictive contraction, the same  $T$  simultaneously calibrates credible intervals and forecast dispersion.

*Implications.* Berk’s theorem is not an exception to Bayesian learning but the boundary case of constrained prediction, with curvature serving as the single control parameter for both efficiency and

robustness. The diagnostic is geometric (inspect  $\lambda_{\min}(H^*)$ ); the remedy is geometric (rescale the metric via tempering); and the consequences are transparent: fast and brittle when curvature is large, slow and robust when curvature is small, and optimally calibrated when curvature is moderated. This unifies misspecification analysis, posterior tempering, and predictive calibration within a single geometric framework. Recent results by McLatchie et al. [44] reinforce this interpretation: as the sample size grows, the temperature of a power posterior becomes asymptotically inconsequential for predictive accuracy, a limiting manifestation of *predictive collapse* that our curvature-adaptive theory quantifies at finite  $n$ .

## 7 Discussion and Outlook

Our framework reveals a single geometric mechanism underlying predictive inference: collapse under constraints is governed by information curvature. The smallest eigenvalue  $\lambda_{\min}(H^*)$  serves as a local rate constant linking Bayesian prediction, empirical likelihood, generalized method of moments, and generalized estimating equations within a unified metric structure. Classical asymptotic results, including Sanov’s theorem [15, 53], log-Sobolev inequalities [42], and variational analyses [8], describe qualitative convergence; the present formulation makes this geometry quantitative, yielding finite-sample rates interpretable directly in curvature terms.

This perspective recasts rather than replaces the foundations laid by Sanov, Le Cam, and the information-geometric tradition. Empirical likelihood and BETEL correspond to conditional inference on the constraint manifold; GMM and GEE represent its optimal quadratic expansions; Berk’s theorem and tempered posteriors illustrate curvature rescaling under misspecification. In all cases, sharper curvature accelerates concentration while flatter curvature yields robustness through slower collapse.

Chernozhukov and Hong [10] reinterpret classical estimators such as GMM through quasi-posteriors, showing that standard estimators emerge as Laplace-type limits of MCMC-based Bayesian updates. Their framework uses MCMC to approximate optimal weighting and curvature. By contrast, the present analysis derives this Gaussian structure directly from first principles—exchangeability and constraint geometry—without recourse to sampling algorithms. The curvature term  $\lambda_{\min}(H^*)$  appears not as a numerical by-product but as the intrinsic geometric rate governing predictive contraction, providing a constructive explanation of the phenomena that quasi-Bayesian methods simulate.

### 7.1 Methodological Implications

Our analysis complements the classical Sanov route by asking the dual question: given empirical constraints, how rapidly does the predictive law return to equilibrium on the constraint manifold? This perspective makes  $\lambda_{\min}(H^*)$  the control parameter for this return, linking information geometry with predictive concentration. The Lanford window construction refines standard saddlepoint expansions by balancing lattice discretization and Gaussian localization, yielding practical non-asymptotic bounds. As the construction is coordinate invariant, the contraction rate depends only on geometric curvature, not parameterization.

## 7.2 Limitations and Future Directions

The analysis rests on two simplifying assumptions: a finite sampling space  $\mathcal{X}$  and full exchangeability. The finite setting enables exact Gaussian control and uniform bounds. Extending to continuous or infinite-dimensional spaces would replace  $\mathbb{T}^*$  with a reproducing-kernel Hilbert space and  $H^*$  with an integral operator, requiring functional-analytic tools and linking to the asymptotic theory of functional inequalities [42].

Exchangeability provides the structural symmetry essential for the inverse Sanov argument. Relaxations such as partial or conditional exchangeability preserve the qualitative form but introduce geometry-dependent normalizations. The framework invites extensions to high-dimensional regimes where the spectrum of  $H^*$  obeys random-matrix laws [4, 29, 57], infinite-dimensional geometries governed by operator curvature, and adaptive settings where  $\dot{H}_t^*$  characterizes stability in online learning. These directions position the present results as a finite, constructive core from which more general measure-theoretic and dynamic theories may develop.

## Acknowledgement

The initial idea for this work originated in 2014 after the authors attended a seminar on Bayesian nonparametrics and the method of moments. It was during that discussion that the possibility of an alternative route, linking predictive asymptotics to constraint geometry, first became apparent. The present framework developed gradually from that early intuition.

## A Proofs of Main Results

### Lanford Windows and Operator–Theoretic Foundation

The Lanford window construction introduced in Section 3 admits an operator–theoretic formulation originally developed by Lanford [35, 36] for lattice gases and combinatorial systems, here adapted to constrained exchangeable sequences. The aim is to formalize the localization principle that balances Gaussian fluctuations against lattice discretization errors.

The Gaussian approximation of Theorem 3.1 is valid for  $O(n^{-1/2})$  fluctuations around the information projection  $P^*$ , while the multinomial lattice introduces discretization errors of comparable order. Setting

$$\rho_n^2 \lambda_{\min}(H^*)/2 = \log n$$

balances these two effects: empirical types farther than  $\rho_n$  from  $P^*$  have exponentially small weight of order  $O(n^{-1})$ , whereas lattice approximation errors within the window  $\mathcal{W}_n$  remain of order  $O(n^{-1/2})$ .

**Definition of the Lanford operator.** For functions  $f : E_n \rightarrow \mathbb{R}$  defined on the set of feasible empirical measures, define the *Lanford operator*

$$\mathcal{L}_n[f](P) = \frac{\sum_{Q \in E_n} f(Q) \exp\left\{-\frac{n}{2}(Q - P^*)^\top H^*(Q - P^*)\right\}}{\sum_{Q \in E_n} \exp\left\{-\frac{n}{2}(Q - P^*)^\top H^*(Q - P^*)\right\}},$$

which maps test functions to their Gaussian-weighted local averages around the information projection  $P^*$ . Here  $H^*$  denotes the information-geometric Hessian at  $P^*$  and  $\lambda_{\min}(H^*)$  its smallest eigenvalue, quantifying local curvature.

**Fixed-point characterization.** Applying  $\mathcal{L}_n$  to the quadratic test function  $f(Q) = \|Q - P^*\|_2^2$  gives the expected squared localization radius,

$$\rho_n^2 = \mathcal{L}_n[\|P - P^*\|_2^2](P^*) = \frac{\sum_{Q \in E_n} \|Q - P^*\|_2^2 \exp\left\{-\frac{n}{2}(Q - P^*)^\top H^*(Q - P^*)\right\}}{\sum_{Q \in E_n} \exp\left\{-\frac{n}{2}(Q - P^*)^\top H^*(Q - P^*)\right\}}.$$

This expression admits a unique fixed point satisfying

$$\rho_n^2 \lambda_{\min}(H^*)/2 = \log n + O(1),$$

and hence

$$\rho_n = \left(\frac{2 \log n}{\lambda_{\min}(H^*)}\right)^{1/2}.$$

The resulting window  $\mathcal{W}_n = \{P \in E_n : \|P - P^*\|_2 \leq \rho_n n^{-1/2}\}$  is therefore *curvature-adaptive*: it expands when the constraint manifold is flat (small  $\lambda_{\min}$ ) and contracts under strong curvature.

**Convergence of the operator iteration.** Iterating the operator  $\mathcal{L}_n$  from any initial radius estimate  $\rho_{n,0}$  yields a contractive mapping

$$\rho_{n,k+1}^2 = \mathcal{L}_n[\|P - P^*\|_2^2](P^*),$$

which converges geometrically to the fixed point at rate  $1 - O(n^{-1/2})$ . This self-consistent localization ensures that the Gaussian approximation remains uniformly valid within  $\mathcal{W}_n$ , providing the analytic foundation for curvature-adaptive predictive collapse.

## A.1 Proof of Theorem 3.1: Tilted Finite Gaussian De Finetti

The argument localizes the predictive mixture around the information projection  $P^*$ , replacing the discrete lattice of feasible empirical types with a Gaussian integral on the tangent space  $\mathbb{T}^*$ . We decompose the constrained predictive sum into interior and exterior contributions relative to the localization window  $\mathcal{W}_n$ :

$$S_n(A) = S_n^{(\text{in})}(A) + S_n^{(\text{out})}(A),$$

where  $S_n^{(\text{in})}(A)$  aggregates empirical types  $P \in \mathcal{W}_n$  and  $S_n^{(\text{out})}(A)$  those with  $P \notin \mathcal{W}_n$ . The exterior component collects types far from the information projection.

**Tail bound.** Recall that

$$\mathcal{W}_n = \{P \in E_n : \|P - P^*\|_2 \leq \rho_n/\sqrt{n}\}, \quad \rho_n^2 = \frac{2 \log n}{\lambda_{\min}(H^*)},$$

where  $\lambda_{\min}(H^*)$  denotes the smallest eigenvalue of the information–geometric Hessian at  $P^*$ .

**Lemma A.1** (Tail control). *For any empirical type  $P \notin \mathcal{W}_n$ ,*

$$\exp\left\{-\frac{n}{2}(P - P^*)^\top H^*(P - P^*)\right\} \leq n^{-1},$$

and consequently

$$|S_n^{(\text{out})}(A)| = O(n^{-1}) \quad \text{uniformly for } A \subset \mathcal{X}^m.$$

*Proof of Lemma A.1.* By convexity of the Kullback–Leibler divergence,

$$D_D(P\|Q) \geq D_D(P^*\|Q) + \frac{1}{2}(P - P^*)^\top H^*(P - P^*).$$

If  $\|P - P^*\|_2 > \rho_n/\sqrt{n}$ , then  $(P - P^*)^\top H^*(P - P^*) \geq \lambda_{\min}(H^*)\rho_n^2/n = 2 \log n/n$ , so the exponential term is bounded by  $n^{-1}$ , proving the claim.  $\square$

**Local expansion inside  $\mathcal{W}_n$ .** For  $P \in \mathcal{W}_n$ , the log–weight admits the quadratic expansion

$$\log \omega_n(P; x_{1:m}) = -nD_D(P^*\|Q) - \frac{n}{2}v^\top H^*v + L_n(v; x_{1:m}) + R_n(v; m),$$

where  $P = P^* + n^{-1/2}v + O(n^{-1})$ ,

$$L_n(v; x_{1:m}) = n^{-1/2} \sum_{i=1}^m v^\top \nabla \log P^*(x_i)$$

is the linear fluctuation term, and  $R_n(v; m) = O(\log n/n^{1/2})$  uniformly for  $\|v\| \leq \rho_n$ . The exponential factor therefore behaves as a Gaussian density on  $\mathbb{T}^*$  with precision  $nH^*$ .

**Discrete–continuous approximation.** Let  $\mathcal{L}_n = \{n^{1/2}(P - P^*) : P \in E_n \cap \mathcal{W}_n\}$  denote the lattice of rescaled deviations.

**Lemma A.2** (Lanford approximation). *For any function  $f$  with a Gaussian envelope,*

$$\sum_{v \in \mathcal{L}_n} f(v) = \int_{\mathbb{T}^* \cap B_{\rho_n}} f(v) dv + O(n^{-1/2} \text{polylog}(n)).$$

*Proof sketch.* The result follows from the localization technique of Lanford [35, 36], which approximates discrete lattice sums by continuous Gaussian integrals over  $\mathbb{T}^*$ , and from standard Laplace approximation techniques for lattice sums [15, 19]. Since the cell volume of the empirical lattice scales as  $n^{-r/2}$  with  $r = \dim(\mathbb{T}^*)$ , the discretization error is  $O(n^{-1/2} \text{polylog } n)$ .  $\square$

**Assembly.** Combining Lemmas A.1 and A.2 gives

$$\mu_{n,m}(A) = \int_{\mathbb{T}^*} P_{P(v)}^{\otimes m}(A) \phi_{H^*}(v) dv + O(n^{-1/2} \text{polylog}(n)),$$

where  $\phi_{H^*}(v)$  is the Gaussian density with precision matrix  $H^*$  and  $P(v) = \Pi(P^* + n^{-1/2}v)$  is the local chart projection onto  $E$ . This establishes Theorem 3.1.

*Remark A.3* (Optimal scaling). The fixed–point radius

$$\rho_n = \left( \frac{2 \log n}{\lambda_{\min}(H^*)} \right)^{1/2}$$

balances the exponentially small tail mass against the  $O(n^{-1/2})$  lattice discretization error, yielding the curvature–sensitive rate  $O(n^{-1/2} \text{polylog } n)$ . This scaling guarantees uniform Gaussian validity while adapting to local curvature: the window expands in flat regions and contracts in highly curved ones.

## A.2 Proof of Theorem 3.4: Predictive Collapse

To bound the total variation distance between the constrained predictive law  $\mu_{n,m}$  and its deterministic limit  $(P^*)^{\otimes m}$ , decompose the expectation according to the localization window  $\mathcal{W}_n$ :

$$\mu_{n,m} = \mathbb{E}[\mathcal{L}(X_{1:m} | P_n) \mathbf{1}_{\mathcal{W}_n}] + \mathbb{E}[\mathcal{L}(X_{1:m} | P_n) \mathbf{1}_{E_n \setminus \mathcal{W}_n}].$$

Here  $\mathcal{W}_n = \{P \in E_n : \|P - P^*\|_2 \leq \rho_n n^{-1/2}\}$  with  $\rho_n^2 = 2 \log n / \lambda_{\min}(H^*)$ , and  $p_{\min}^* = \min_x P^*(x) > 0$ .

Inside  $\mathcal{W}_n$ , two finite-sample deviations contribute to the total variation error: (i) the hypergeometric correction between sampling with and without replacement, and (ii) the local Gaussian deviation between  $P_n$  and  $P^*$ .

The first satisfies

$$\|\mathcal{L}(X_{1:m} | P_n) - P_n^{\otimes m}\|_{\text{TV}} \leq \frac{m(m-1)}{2n p_{\min}^*},$$

by Lemma A.4. The second obeys

$$\|P_n^{\otimes m} - (P^*)^{\otimes m}\|_{\text{TV}} \leq m \sqrt{|\mathcal{X}|} \rho_n n^{-1/2},$$

from the Gaussian localization of Theorem 3.1. The complement  $E_n \setminus \mathcal{W}_n$  contributes  $O(n^{-1})$  by Lemma A.1. Combining these estimates and substituting  $\rho_n^2 = 2 \log n / \lambda_{\min}(H^*)$  yields

$$\|\mu_{n,m} - (P^*)^{\otimes m}\|_{\text{TV}} = O\left(m \sqrt{\frac{\log n}{n \lambda_{\min}(H^*)}} + \frac{m^2}{n p_{\min}^*}\right),$$

which proves Theorem 3.4.

**Lemma A.4** (Hypergeometric bound). *If  $\min_x P(x) > 0$ , then for all  $m \leq n$ ,*

$$\|\mathcal{L}(X_{1:m} | P_n = P) - P^{\otimes m}\|_{\text{TV}} \leq \frac{m(m-1)}{2n p_{\min}},$$

*uniformly for  $P \in \mathcal{P}_n$ .*

*Proof of Lemma A.4.* Under sampling without replacement, each pair of draws introduces a dependence of order  $1/n$ . Bounding the covariance between indicator variables  $\mathbf{1}\{X_i = x\}$  and  $\mathbf{1}\{X_j = y\}$  yields  $\|\mathcal{L}(X_{1:m} | P_n = P) - P^{\otimes m}\|_{\text{TV}} \leq m(m-1)/(2n p_{\min})$ , as in standard finite-population coupling arguments.  $\square$

### A.3 Proof of Corollary 4.1: LAN

By Theorem 3.1, the empirical measure satisfies

$$P_n = P^* + n^{-1/2}Z + O_p(n^{-1}), \quad Z \sim \mathcal{N}(0, (H^*)^{-1}) \text{ on } \mathbb{T}^*.$$

A second-order expansion of the log-density ratio gives

$$\log \frac{d\mu_{n,m}}{d(P^*)^{\otimes m}}(X_{n+1:n+m}) = \Delta_n^\top \xi_m - \frac{1}{2} \Delta_n^\top H^* \Delta_n + o_p(1),$$

where  $\Delta_n = \sqrt{n}(P_n - P^*)$  and  $\xi_m$  is Gaussian with covariance  $(H^*)^{-1}$ . This is the classical LAN expansion of Le Cam and Yang [40], van der Vaart [58], showing that  $\mu_{n,m}$  and  $(P^*)^{\otimes m}$  are contiguous, and completing the proof of Corollary 4.1.

*Remark A.5* (Historical significance). Corollary 4.1 provides a finite predictive analogue of Le Cam’s local asymptotic normality within the discrete, exchangeable setting of this paper. Where classical LAN theory describes the limiting behavior of parametric likelihoods, this result derives the same quadratic expansion from the geometry of constrained exchangeability. The construction recovers Le Cam’s experiment as the limit of a finite predictive law, linking de Finetti’s representation to the Le Cam–Hájek framework through curvature as the common invariant.

## B Auxiliary Results and Curvature Computation

**Lemma B.1** (Existence and uniqueness of the I-projection). *If  $Q(x) > 0$  for all  $x$  and the affine constraint  $AP = \alpha$  is feasible, then*

$$P^* = \arg \min_{P \in E} D_D(P \| Q)$$

*exists and is unique. Moreover,  $P^*(x) > 0$  for all  $x$ , and the associated Lagrange multiplier  $\theta^*$  satisfies  $P^*(x) \propto Q(x) \exp(-\theta^{*\top} A_x)$ .*

**Lemma B.2** (Computing curvature). *Let  $V$  be an orthonormal basis for  $\text{Null}([\mathbf{1}, A^\top])$ . Then the information-geometric Hessian restricted to the tangent space  $\mathbb{T}^*$  is*

$$H^* = V^\top \text{diag}\left(\frac{1}{P^*}\right) V,$$

*and its smallest eigenvalue  $\lambda_{\min}(H^*) = \min_{\|v\|_2=1, v \in \mathbb{T}^*} v^\top H^* v$  quantifies local curvature of the constraint manifold.*

**Theorem B.3** (Tracial and spectral bounds for curvature). *Let  $H^*$  be the positive-definite matrix in Lemma B.2 with eigenvalues  $\lambda_1 \geq \dots \geq \lambda_r > 0$ . Then*

$$\begin{aligned} (i) \quad & \lambda_{\min}(H^*) \geq \frac{r}{\text{tr}\{(H^*)^{-1}\}}, \\ (ii) \quad & \frac{1}{\text{tr}(H^*)} \leq \frac{\lambda_{\min}(H^*)}{r} \leq \frac{\lambda_{\min}(H^*)}{\lambda_{\max}(H^*)}, \\ (iii) \quad & \text{tr}(H^*) = \sum_{x \in \mathcal{X}} \frac{\|V_x\|_2^2}{P^*(x)}, \quad \det(H^*) = \det(V^\top \text{diag}(1/P^*)V). \end{aligned}$$

*Equality in (i) holds iff all nonzero eigenvalues are equal (isotropic geometry). The trace and determinant of  $H^*$  provide coarse but computable proxies for  $\lambda_{\min}(H^*)$ .*

**Theorem B.4** (Numerical stability). *Let  $\widehat{P}^*$  satisfy  $\|\nabla L(\widehat{P}^*)\| \leq n^{-1/2}$ . Then, by Weyl's inequality,  $|\widehat{\lambda}_{\min} - \lambda_{\min}(H^*)| = O(n^{-1/2})$ .*

*Remark B.5* (Practical computation). Compute  $\lambda_{\min}(H^*)$  via SVD/eigen-decomposition of the Jacobian restricted to  $\mathbb{T}^*$ . Bootstrap variability is  $O(n^{-1/2})$ , and  $r/\text{tr}\{(H^*)^{-1}\}$  provides a stable proxy when  $r$  is large.

## C GMM, GEE, and Berk's Theorem

### C.1 Proof of Theorem 5.3: GMM optimality

Let  $\bar{g}_n(\theta) = n^{-1} \sum_i g(X_i, \theta)$  denote the sample moment and  $A_\theta = \partial_\theta \mathbb{E}[g(X, \theta)]$  the Jacobian of the population moment condition. By Theorem 3.1, the conditional law of empirical types near  $P_\theta^*$  is Gaussian on the tangent space  $\mathbb{T}_\theta^*$  with precision matrix  $H_\theta^*$ . Writing  $P = P_\theta^* + n^{-1/2}V_\theta v$ , with  $V_\theta$  a basis for  $\mathbb{T}_\theta^*$ , gives the local expansion

$$A_\theta P = \alpha(\theta) + n^{-1/2}A_\theta V_\theta v + o(n^{-1/2}),$$

where  $\alpha(\theta) = \mathbb{E}[g(X, \theta)]$ . Conditioning on the empirical constraint  $\bar{g}_n(\theta) = 0$  enforces  $A_\theta V_\theta v = \sqrt{n} \bar{g}_n(\theta) + o_p(1)$ . Because the conditional density of  $v$  is proportional to  $\exp\{-\frac{1}{2}v^\top H_\theta^* v\}$ , the likelihood is maximized at the minimal-energy solution of this constraint. Substituting the implied  $v$  yields

$$-\log \mathcal{L}_{\text{cond}}(\theta) = \frac{n}{2} \bar{g}_n(\theta)^\top \left[ (A_\theta|_{\mathbb{T}_\theta^*}) H_\theta^{*-1} (A_\theta|_{\mathbb{T}_\theta^*})^\top \right]^{-1} \bar{g}_n(\theta) + O_p(n^{-1/2}),$$

which coincides with the GMM criterion up to a curvature-weighted quadratic form. Hence GMM is the optimal quadratic expansion of the conditional (BETEL) likelihood.

### C.2 Proof of Theorem 5.4: GEE robustness

Let

$$U_n(\theta) = n^{-1} \sum_i D_i(\theta)^\top W_i(\theta) \{Y_i - \mu_i(\theta)\},$$

where  $D_i(\theta) = \partial_\theta \mu_i(\theta)$  and  $W_i(\theta)$  are working weights. Let  $\theta_0$  solve  $\mathbb{E}[U_n(\theta_0)] = 0$ . A Taylor expansion gives  $\|U_n(\theta_0)\| = O_p(\sqrt{\log n/n})$  and  $H_n(\hat{\theta}) \rightarrow J(\theta_0) = \mathbb{E}[D_i^\top W_i D_i]$ . Consequently,

$$\|\hat{\theta} - \theta_0\| = O_p\left(\sqrt{\frac{\log n}{n \lambda_{\min}\{J(\theta_0)\}}}\right).$$

If  $aH_{\theta_0}^* \preceq J(\theta_0) \preceq bH_{\theta_0}^*$  for constants  $0 < a < b < \infty$ , then  $\lambda_{\min}\{J(\theta_0)\} \geq a \lambda_{\min}(H_{\theta_0}^*)$ , and the same curvature-controlled rate follows up to factor  $a^{-1/2}$ . Asymptotic normality holds by the Lindeberg–Feller theorem, showing that curvature again governs robustness and rate of convergence.

### C.3 Proof of Theorem 6.1 and Corollary 6.2: Berk’s Theorem and Prediction Bound

By the finite-sample LAN expansion of Corollary 4.1, the posterior law of  $\Delta_n = \sqrt{n}(\theta - \theta_0)$  satisfies

$$\log \frac{d\Pi_n}{d\Pi_0}(\theta) = \ell_n(\theta) - \ell_n(\theta_0) = \Delta_n^\top \xi_n - \frac{1}{2} \Delta_n^\top H_{\theta_0}^* \Delta_n + o_p(1),$$

where  $\xi_n \sim \mathcal{N}(0, (H_{\theta_0}^*)^{-1})$  and  $H_{\theta_0}^*$  is the information–geometric Hessian at  $\theta_0$ . Applying a Chernoff bound to this quadratic form yields

$$\Pr(\|\theta - \theta_0\|_2 > \varepsilon \mid X_{1:n}) \leq C \exp\{-c n \lambda_{\min}(H_{\theta_0}^*) \varepsilon^2\},$$

for constants  $c, C > 0$  depending on local geometry and the prior, which proves Theorem 6.1.

The predictive version (Corollary 6.2) follows by substituting this contraction rate into Theorem 3.4, yielding

$$\|\mu_{n,m} - (P_{\theta_0}^*)^{\otimes m}\|_{\text{TV}} = O\left(m \sqrt{\frac{\log n}{n \lambda_{\min}(H_{\theta_0}^*)}}\right),$$

for  $m = o(\sqrt{n \lambda_{\min}(H_{\theta_0}^*)/\log n})$ . This completes the proofs of Theorem 6.1 and Corollary 6.2.

*Remark C.1* (Historical note). Berk’s 1966 theorem marked a turning point: it showed that Bayesian posteriors remain coherent even when the model is false, converging to the pseudo-true parameter rather than to truth itself. The present formulation extends this insight from asymptotic inevitability to finite predictive geometry. It shows that misspecification is not merely stochastic error but geometric distortion: curvature, not contradiction, governs how belief collapses around a useful fiction. In this sense, Berk’s result was not an exception to Bayesian learning but its first cautionary proof that convergence alone does not imply understanding.

## References

- [1] D. J. Aldous. Exchangeability and related topics. In P.-L. Hennequin, editor, *École d’Été de Probabilités de Saint-Flour XIII—1983*, volume 1117 of *Lecture Notes in Mathematics*, pages 1–198. Springer, Berlin, 1985. doi: 10.1007/BFb0099420.

- [2] S. Amari. *Information Geometry and Its Applications*. Springer, Tokyo, 2016. doi: 10.1007/978-4-431-55978-8.
- [3] S. Amari and H. Nagaoka. *Methods of Information Geometry*, volume 191 of *Translations of Mathematical Monographs*. American Mathematical Society, Providence, 2000. doi: 10.1090/mmono/191.
- [4] J. Baik, G. Ben Arous, and S. Péché. Phase transition of the largest eigenvalue for nonnull complex sample covariance matrices. *The Annals of Probability*, 33(5):1643–1697, 2005. doi: 10.1214/009117905000000233.
- [5] R. H. Berk. Limiting behavior of posterior distributions when the model is incorrect. *The Annals of Mathematical Statistics*, 37(1):51–58, 1966. doi: 10.1214/aoms/1177699597.
- [6] M. Berta, L. Gavalakis, and I. Kontoyiannis. A third information-theoretic approach to finite de finetti theorems. In *2024 IEEE International Symposium on Information Theory (ISIT)*, pages 73–78. IEEE, 2024. doi: 10.1109/ISIT57864.2024.10619572.
- [7] P. G. Bissiri, C. C. Holmes, and S. G. Walker. A general framework for updating belief distributions. *Journal of the Royal Statistical Society: Series B (Statistical Methodology)*, 78(5):1103–1130, 2016. doi: 10.1111/rssb.12158.
- [8] D. M. Blei, A. Kucukelbir, and J. D. McAuliffe. Variational inference: A review for statisticians. *Journal of the American Statistical Association*, 112(518):859–877, 2017. doi: 10.1080/01621459.2017.1285773.
- [9] L. D. Brown. *Fundamentals of Statistical Exponential Families: With Applications in Statistical Decision Theory*, volume 9 of *Lecture Notes-Monograph Series*. Institute of Mathematical Statistics, Hayward, 1986. doi: 10.1214/lnms/1215540309.
- [10] V. Chernozhukov and H. Hong. An mcmc approach to classical estimation. *Journal of Econometrics*, 115(2):293–346, 2003. doi: 10.1016/S0304-4076(03)00100-3.
- [11] S. Chib, M. Shin, and A. Simoni. Bayesian estimation and comparison of moment condition models. *Journal of the American Statistical Association*, 113(524):1656–1668, 2018. doi: 10.1080/01621459.2017.1358172.
- [12] S. Chib, M. Shin, and A. Simoni. Bayesian estimation and comparison of conditional moment models. *Journal of the Royal Statistical Society: Series B (Statistical Methodology)*, 84(3):740–764, 2022. doi: 10.1111/rssb.12484.
- [13] I. Csiszár. I-divergence geometry of probability distributions and minimization problems. *The Annals of Probability*, 3(1):146–158, 1975. doi: 10.1214/aop/1176996454.
- [14] B. de Finetti. La prévision: Ses lois logiques, ses sources subjectives. *Annales de l’Institut Henri Poincaré*, 7(1):1–68, 1937.
- [15] A. Dembo and O. Zeitouni. *Large Deviations Techniques and Applications*. Springer, New York, 2nd edition, 1998. doi: 10.1007/978-1-4612-5320-4.

- [16] P. Diaconis and D. Freedman. De finetti's theorem for markov chains. *The Annals of Probability*, 8(1):115–130, 1980. doi: 10.1214/aop/1176994828.
- [17] P. Diaconis and D. Freedman. A dozen de finetti-style results in search of a theory. *Annales de l'Institut Henri Poincaré, Probabilités et Statistiques*, 23(2):397–423, 1987.
- [18] J. L. Doob. Application of the theory of martingales. *Colloques Internationaux du Centre National de la Recherche Scientifique*, 13:23–27, 1949. Reprinted in Selected Papers of J. L. Doob, eds. L. Breiman and D. Freedman, American Mathematical Society, 1980.
- [19] R. S. Ellis. *Entropy, Large Deviations, and Statistical Mechanics*. Springer, New York, 2006. doi: 10.1007/978-3-540-29060-5.
- [20] V. P. Godambe. An optimum property of regular maximum likelihood estimation. *The Annals of Mathematical Statistics*, 31(4):1208–1211, 1960. doi: 10.1214/aoms/1177705689.
- [21] V. P. Godambe. The foundations of finite sample estimation in stochastic processes. *Biometrika*, 72(2):419–428, 1985. doi: 10.1093/biomet/72.2.419.
- [22] P. D. Grünwald. The safe bayesian: Learning the learning rate via the mixability gap. *Journal of Machine Learning Research*, 13(1):3075–3099, 2012.
- [23] L. P. Hansen. Large sample properties of generalized method of moments estimators. *Econometrica*, 50(4):1029–1054, 1982. doi: 10.2307/1912775.
- [24] D. Heath and W. D. Sudderth. On finitely additive priors, coherence, and extended admissibility. *The Annals of Statistics*, 6(2):333–345, 1978. doi: 10.1214/aos/1176344128.
- [25] C. C. Holmes and S. G. Walker. Assigning a value to a power likelihood in a general bayesian model. *Biometrika*, 104(2):497–503, 2017. doi: 10.1093/biomet/asx010.
- [26] P. J. Huber. The behavior of maximum likelihood estimates under nonstandard conditions. *Proceedings of the Fifth Berkeley Symposium on Mathematical Statistics and Probability*, 1: 221–233, 1967.
- [27] G. W. Imbens, R. H. Spady, and P. Johnson. Information theoretic approaches to inference in moment condition models. *Econometrica*, 66(2):333–357, 1998. doi: 10.2307/2998561.
- [28] E. T. Jaynes. Information theory and statistical mechanics. *Physical Review*, 106(4):620–630, 1957. doi: 10.1103/PhysRev.106.620.
- [29] K. Johansson. Shape fluctuations and random matrices. *Communications in Mathematical Physics*, 209(2):437–476, 2000. doi: 10.1007/s002200050027.
- [30] R. E. Kass. Statistical inference: The big picture. *Statistical Science*, 26(1):1–9, 2011. doi: 10.1214/10-STSS337.
- [31] R. E. Kass and P. W. Vos. *Geometrical Foundations of Asymptotic Inference*. Wiley Series in Probability and Statistics. John Wiley & Sons, New York, 1997. ISBN 978-0-471-82668-2. doi: 10.1002/9781118165973.

- [32] Y. Kitamura. Empirical likelihood methods with weakly dependent processes. *The Annals of Statistics*, 25(5):2084–2102, 1997. doi: 10.1214/aos/1069362388.
- [33] B. J. K. Kleijn and A. W. van der Vaart. Misspecification in infinite-dimensional bayesian statistics. *The Annals of Statistics*, 34(2):837–877, 2006. doi: 10.1214/009053606000000029.
- [34] B. J. K. Kleijn and A. W. van der Vaart. The bernstein–von mises theorem under misspecification. *Electronic Journal of Statistics*, 6:354–381, 2012. doi: 10.1214/12-EJS675.
- [35] O. E. Lanford. Entropy and equilibrium states in classical statistical mechanics. In A. Lenard, editor, *Statistical Mechanics and Mathematical Problems*, volume 20 of *Lecture Notes in Physics*, pages 1–113. Springer, Berlin, 1973. doi: 10.1007/BFb0112756.
- [36] O. E. Lanford. Time evolution of large classical systems. In J. Moser, editor, *Dynamical Systems, Theory and Applications*, volume 38 of *Lecture Notes in Physics*, pages 1–111. Springer, Berlin, 1978. doi: 10.1007/BFb0015382.
- [37] N. A. Lazar. A review of empirical likelihood. *Annual Review of Statistics and Its Application*, 8:329–344, 2021. doi: 10.1146/annurev-statistics-040720-024710.
- [38] N. A. Lazar and P. A. Mykland. An evaluation of the power and conditionality properties of empirical likelihood. *Biometrika*, 85(3):523–534, 1998. doi: 10.1093/biomet/85.3.523.
- [39] L. Le Cam. Limits of experiments. *Proceedings of the Sixth Berkeley Symposium on Mathematical Statistics and Probability*, 1:245–261, 1972.
- [40] L. Le Cam and G. L. Yang. *Asymptotics in Statistics: Some Basic Concepts*. Springer, New York, 2nd edition, 2000. doi: 10.1007/978-1-4612-1166-2.
- [41] L. M. Le Cam. *Asymptotic Methods in Statistical Decision Theory*. Springer Series in Statistics. Springer, New York, 1986. doi: 10.1007/978-1-4612-4946-7.
- [42] M. Ledoux. *The Concentration of Measure Phenomenon*, volume 89 of *Mathematical Surveys and Monographs*. American Mathematical Society, Providence, 2001. ISBN 978-0-8218-2864-9. doi: 10.1090/surv/089.
- [43] K.-Y. Liang and S. L. Zeger. Longitudinal data analysis using generalized linear models. *Biometrika*, 73(1):13–22, 1986. doi: 10.1093/biomet/73.1.13.
- [44] Y. McLatchie, E. Fong, D. T. Frazier, and J. Knoblauch. Predictive performance of power posteriors. *Biometrika*, 112(3):asaf034, 2025. doi: 10.1093/biomet/asaf034. URL <https://arxiv.org/abs/2408.08806>.
- [45] J. F. Monahan and D. D. Boos. Proper likelihoods for bayesian analysis. *Biometrika*, 79(2):271–278, 1992. doi: 10.1093/biomet/79.2.271.
- [46] W. K. Newey and D. L. McFadden. Large sample estimation and hypothesis testing. In R. F. Engle and D. L. McFadden, editors, *Handbook of Econometrics*, volume 4 of *Handbooks in Economics*, pages 2111–2245. Elsevier, Amsterdam, 1994. doi: 10.1016/S1573-4412(05)80005-4.

- [47] W. K. Newey and R. J. Smith. Higher order properties of gmm and generalized empirical likelihood estimators. *Econometrica*, 72(1):219–255, 2004. doi: 10.1111/j.1468-0262.2004.00482.x.
- [48] F. Nielsen. An elementary introduction to information geometry. *Entropy*, 22(10):1100, 2020. doi: 10.3390/e22101100.
- [49] A. B. Owen. Empirical likelihood ratio confidence intervals for a single functional. *Biometrika*, 75(2):237–249, 1988. doi: 10.1093/biomet/75.2.237.
- [50] A. B. Owen. *Empirical Likelihood*. Chapman and Hall/CRC, Boca Raton, 2001. doi: 10.1201/9781420036152.
- [51] N. G. Polson and D. Zantedeschi. De finetti + sanov = bayes. *arXiv preprint arXiv:2509.13283*, 2025. doi: 10.48550/arXiv.2509.13283. URL <https://arxiv.org/abs/2509.13283>.
- [52] J. Qin and J. Lawless. Empirical likelihood and general estimating equations. *The Annals of Statistics*, 22(1):300–325, 1994. doi: 10.1214/aos/1176325360.
- [53] I. N. Sanov. On the probability of large deviations of random variables. *Matematicheskii Sbornik*, 42(84):11–44, 1957. In Russian; English translation in Selected Translations in Mathematical Statistics and Probability, vol. 1, pp. 213–244, American Mathematical Society, Providence, 1961.
- [54] S. M. Schennach. Point estimation with exponentially tilted empirical likelihood. *The Annals of Statistics*, 35(2):634–672, 2007. doi: 10.1214/009053606000001208.
- [55] Susanne M. Schennach. Bayesian exponentially tilted empirical likelihood. *Biometrika*, 92(1):31–46, 2005. doi: 10.1093/biomet/92.1.31.
- [56] N. Syring and R. Martin. Calibrating general posterior credible regions. *Biometrika*, 106(2):479–486, 2019. doi: 10.1093/biomet/asz006.
- [57] C. A. Tracy and H. Widom. Level-spacing distributions and the airy kernel. *Communications in Mathematical Physics*, 159(1):151–174, 1994. doi: 10.1007/BF02100489.
- [58] A. W. van der Vaart. *Asymptotic Statistics*. Cambridge University Press, Cambridge, 1998. doi: 10.1017/CBO9780511802256.
- [59] H. White. Maximum likelihood estimation of misspecified models. *Econometrica*, 50(1):1–25, 1982. doi: 10.2307/1912526.